AFRL-RY-WP-TP-2008-1160

COMPARATIVE STUDY OF COHERENT, NON-COHERENT, AND SEMI-COHERENT INTEGRATION SCHEMES FOR GNSS RECEIVERS (PREPRINT)

Chun Yang, Mikel Miller, Erik Blasch, and Thao Nguyen

Sigtem Technology, Inc.

APRIL 2007

Approved for public release; distribution unlimited.

See additional restrictions described on inside pages

STINFO COPY

AIR FORCE RESEARCH LABORATORY
SENSORS DIRECTORATE
WRIGHT-PATTERSON AIR FORCE BASE, OH 45433-7320
AIR FORCE MATERIEL COMMAND
UNITED STATES AIR FORCE

REPORT DOCUMENTATION PAGE

Form Approved
OMB No. 0704-0188

The public reporting burden for this collection of information is estimated to average 1 hour per response, including the time for reviewing instructions, searching existing data sources, searching existing data sources, gathering and maintaining the data needed, and completing and reviewing the collection of information. Send comments regarding this burden estimate or any other aspect of this collection of information, including suggestions for reducing this burden, to Department of Defense, Washington Headquarters Services, Directorate for Information Operations and Reports (0704-0188), 1215 Jefferson Davis Highway, Suite 1204, Arlington, VA 22202-4302. Respondents should be aware that notwithstanding any other provision of law, no person shall be subject to any penalty for failing to comply with a collection of information if it does not display a currently valid OMB control number. **PLEASE DO NOT RETURN YOUR FORM TO THE ABOVE ADDRESS**.

1. REPORT DATE *(DD-MM-YY)*	2. REPORT TYPE	3. DATES COVERED *(From - To)*
April 2007	Conference Paper Preprint	08 April 2005 – 08 April 2007

4. TITLE AND SUBTITLE
COMPARATIVE STUDY OF COHERENT, NON-COHERENT, AND SEMI-COHERENT INTEGRATION SCHEMES FOR GNSS RECEIVERS (PREPRINT)

5a. CONTRACT NUMBER
FA8650-05-C-1828

5b. GRANT NUMBER

5c. PROGRAM ELEMENT NUMBER
65502F

6. AUTHOR(S)
Chun Yang (Sigtem Technology, Inc.)
Mikel Miller and Thao Nguyen (AFRL/RYRN)
Erik Blasch (AFRL/RYAA)

5d. PROJECT NUMBER
3005

5e. TASK NUMBER
13

5f. WORK UNIT NUMBER
300513CY

7. PERFORMING ORGANIZATION NAME(S) AND ADDRESS(ES)
Sigtem Technology, Inc.
1343 Parrott Drive
San Mateo, CA 94402-3630

Reference Systems Branch (AFRL/RYRN)
RF Sensor Technology Division
Assessment and Integration Branch (AFRL/RYAA)
Sensor ATR Technology Division
Air Force Research Laboratory, Sensors Directorate
Wright-Patterson Air Force Base, OH 45433-7320
Air Force Materiel Command, United States Air Force

8. PERFORMING ORGANIZATION REPORT NUMBER

9. SPONSORING/MONITORING AGENCY NAME(S) AND ADDRESS(ES)
Air Force Research Laboratory
Sensors Directorate
Wright-Patterson Air Force Base, OH 45433-7320
Air Force Materiel Command
United States Air Force

10. SPONSORING/MONITORING AGENCY ACRONYM(S)
AFRL/RYRN

11. SPONSORING/MONITORING AGENCY REPORT NUMBER(S)
AFRL-RY-WP-TP-2008-1160

12. DISTRIBUTION/AVAILABILITY STATEMENT
Approved for public release; distribution unlimited.

13. SUPPLEMENTARY NOTES
Paper produced under contract FA8650-05-C-1828 for technical report AFRL-RY-WP-TR-2008-1137, SOFTWARE TOOLKIT FOR NONLINEAR FILTERS FOR GLOBAL POSITIONING SYSTEM (GPS) OPERATIONAL CONTROL SEGMENT (OCS) ESTIMATION AND OTHER APPLICATIONS.

Conference paper published in the Proceedings of the Annual Meeting - Institute of Navigation, 63rd Annual Meeting of the Institute of Navigation 2007, Apr 23-25 2007, held in Cambridge, MA; Publisher: Institute of Navigation.

PAO Case Number: SN 06-0404; Clearance date: 20 December 2006. The U.S. Government is joint author of this work and has the right to use, modify, reproduce, release, perform, display, or disclose the work. Paper contains color.

14. ABSTRACT
Three integration schemes, namely, coherent, non-coherent, and semi-coherent integration, and their variants are described in this paper for signal detection and tracking in such applications as pulsed Doppler radar and GPS receiver. We adopt a unified approach to present such integration schemes as best approximations to the likelihood ratio test (LRT) when the signal models are partially known to different extents. Formulas for the conditional probability density functions (pdfs) of the sufficient statistic under alternative hypotheses as well as the probability of detection (P_d) and probability of false alarm (P_{fa}) are given. Integration improvement factors and integration losses are then formulated. Connections of the semi-coherent integration scheme to the cyclic auto-correlation function, the discrete-time Wigner-Ville transform, and the radar ambiguity function are also outlined. *Abstract concludes on reverse side* →

15. SUBJECT TERMS

16. SECURITY CLASSIFICATION OF:			17. LIMITATION OF ABSTRACT:	18. NUMBER OF PAGES	19a. NAME OF RESPONSIBLE PERSON (Monitor)
a. REPORT	b. ABSTRACT	c. THIS PAGE			Thao Nguyen
Unclassified	Unclassified	Unclassified	SAR	24	19b. TELEPHONE NUMBER *(Include Area Code)* N/A

14. ABSTRACT (concluded)

Although most of the results are available in the literature, they are scattered in different textbooks and research papers. By presenting them in a cohesive and concise manner, the paper can serve as (1) an introductory material with key references for those who would like to study the subject further, (2) a quick reference for those who would like to compare these integration schemes, and (3) an integrated approach under varying conditions. Simulation results are presented to compare these integration schemes in terms of detection performance (P_d and P_{fa}) as a function of signal-to-noise ratio (SNR) and integration interval under two operating conditions. One is for a signal with constant Doppler frequency and the other is for a linear frequency modulation signal (i.e., a chirp signal). We show the curves of the input SNR required under different chirp rates so as to maintain the same detection performance, the resulting LRTs for the different approaches, as well as simulated comparisons between tradeoffs of P_d versus *SNR*.

Comparative Study of Coherent, Non-Coherent, And Semi-Coherent Integration Schemes For GNSS Receivers

Chun Yang
Sigtem Technology, Inc

Mikel Miller
Air Force Research Lab/SNRN

Erik Blasch
Air Force Research Lab/SNAA

Thao Nguyen
Air Force Research Lab/SNRN

BIOGRAPHIES

Dr. Chun Yang received his title of Docteur en Science from the Université de Paris (No. XI, Orsay), France, in 1989. After two years of post-doctoral research at the University of Connecticut, he moved on with his industrial R&D career. Since 1993, he has been with Sigtem Technology, Inc. and has been working on numerous GPS, integrated inertial, and adaptive array related projects. He is the co-inventor of seven issued or pending U.S. patents. He is also an Adjunct Professor of Electrical and Computer Engineering at Miami University of Ohio.

Dr. Mikel Miller is the Technical Advisor for the Reference Systems Branch, Sensors Directorate, Air Force Research Laboratory, WPAFB, OH. He received his Ph.D. in Electrical Engineering from the Air Force Institute of Technology (AFIT), WPAFB, Ohio, in 1998. Since 1986, he has focused on navigation system R&D related to GPS, GPS/INS integrations, alternative navigation techniques including bio-inspired navigation and signals of opportunity based navigation, autonomous vehicle navigation and control, and multi-sensor fusion. He is currently responsible for both in-house and contracted R&D projects advancing navigation technology. He is also an Adjunct Professor of EE at AFIT and Miami University of Ohio. Dr. Miller is a member of the ION, RIN, IEEE, and AIAA.

Dr. Erik Blasch is a Fusion Evaluation Tech Lead for the Assessment & Integration Branch, Sensors Directorate, Air Force Research Laboratory, WPAFB, OH. He is an adjunct professor at Wright State University (WSU)/ University of Dayton (UD)/AFIT and a Reserve Major at the Air Force Office of Scientific Research (AFOSR). He received his Ph.D. in Electrical Engineering from WSU in 1999, a MSEE from WSU in 1997, a MSME from Georgia Tech in 1994, and a BSME from MIT in 1992 among other advanced degrees in engineering, health science, economics, and business administration. He is the President of the International Society of Information Fusion (ISIF) and active in IEEE, SPIE, and ION. His research interests include target tracking, sensor fusion, automatic target recognition, biologically-inspired robotics, and controls.

Thao Nguyen is a Ph.D. candidate in the Electrical and Computer Engineering Department at the Air Force Institute of Technology (AFIT), Wright-Patterson AFB, Ohio. He also works as an Electronics Engineer at the Reference Systems Branch, Sensors Directorate, Air Force Research Laboratory, WPAFB, OH. Mr. Nguyen has been involved with navigation-related research, development, and test since 2002 and his current areas of interest include high anti-jamming technologies for GPS receivers, GPS/INS integration, multi-sensor fusion, and personal navigation using signals of opportunity (SoOP).

ABSTRACT

Three integration schemes, namely, coherent, non-coherent, and semi-coherent integration, and their variants are described in this paper for signal detection and tracking in such applications as pulsed Doppler radar and GPS receiver. We adopt a unified approach to present such integration schemes as best approximations to the likelihood ratio test (LRT) when the signal models are partially known to different extents. Formulas for the conditional probability density functions (pdfs) of the sufficient statistic under alternative hypotheses as well as the probability of detection (P_d) and probability of false alarm (P_{fa}) are given. Integration improvement factors and integration losses are then formulated. Connections of the semi-coherent integration scheme to the cyclic autocorrelation function, the discrete-time Wigner-Ville transform, and the radar ambiguity function are also outlined. Although most of the results are available in the literature, they are scattered in different textbooks and research papers. By presenting them in a cohesive and

concise manner, the paper can serve as (1) an introductory material with key references for those who would like to study the subject further, (2) a quick reference for those who would like to compare these integration schemes, and (3) an integrated approach under varying conditions. Simulation results are presented to compare these integration schemes in terms of detection performance (P_d and P_{fa}) as a function of signal to noise ratio (SNR) and integration interval under two operating conditions. One is for a signal with constant Doppler frequency and the other is for a linear frequency modulation signal (*i.e.*, a chirp signal). We show the curves of the input SNR required under different chirp rates so as to maintain the same detection performance, the resulting LRTs for the different approaches, as well as simulated comparisons between trade-offs of P_d versus *SNR*.

INTRODUCTION

In this paper, we study several integration schemes frequently encountered for signal detection and parameter estimation in such applications as pulsed Doppler radar and GPS receivers. The signals employed in these two fields are quite different in their operating modes and waveforms (*e.g.*, frequencies, modulations and power levels). Even different names are given to similar integration schemes: pulse integration for radar vs. post-correlation integration for GPS. Nevertheless, the principles and methodologies are common and our goal is to integrate the approaches toward advanced detection capabilities. For an experienced reader, he or she may go directly to the section *Simulation Results and Analysis* that highlights the comparative study.

For a signal buried in noise, a single signal sample is typically not suitable for detection simply because the signal in such raw samples is too weak (*i.e.*, low SNR) at a high sampling rate. To improve detection performance, multiple successive samples are therefore processed jointly, which also serves the purpose of data compression. In a pulsed Doppler radar, a pulse-matched filter is applied to signal samples to accumulate the signal energy per pulse while averaging out noise. Similarly, in a GPS receiver, a despreading correlator is applied to signal samples per code epoch, which is 1 ms long for GPS C/A-codes. The resulting measurement per pulse or per code epoch is typically complex-valued, containing real and imaginary parts, also known as in-phase and quadrature-phase components.

Pulse measurements in radar or pre-detection correlations in GPS are further processed before a decision is made to ascertain the presence or absence of a desired signal. Decision making is carried out by means of threshold comparison and detection performance is characterized in terms of probability of detection (P_d) and probability of false alarm (P_{fa}) for a detection threshold. One way to optimally process these measurements is to reduce them into a sufficient statistic, denoted by λ. Under different conditions, this leads to different integration schemes, which are the subject of study in this paper.

Indeed, we choose a unified way to present various measurement-combining (or integration) schemes as the best approximation by a sufficient statistic of the likelihood ratio test (LRT) resulting from hypothesis testing when the underlying signal model is partially known to a different degree. There are two hypotheses of interest. One is the null hypothesis, denoted by H_0, under which measurement only contains noise. The other is the alternative hypothesis, denoted by H_1, under which the signal of interest is present in the noisy measurement. Once a sufficient statistic is given, a major step that follows is to derive the conditional probability density functions (pdfs) of the sufficient statistic under the two hypotheses, namely, $P(\lambda|H_0)$ and $P(\lambda|H_1)$, respectively, from which P_d and P_{fa} are evaluated for a given threshold. When closed-form solutions are not available, empirical formulas and numerical/graphic means are often used to facilitate design and implementation.

Coherent integration (here "coherent" means matched in time/phase) works on complex-valued measurements in which the signal's phases from measurement to measurement are in close alignment, thus allowing constructive addition of signal whereas the phase of noise is random from measurement to measurement, resulting in cancellation. Coherent integration can attain the highest integration gain ideally (100% efficiency). To achieve a build up of signal amplitude, the phase relationship between measurements has to be known or estimated, which is, however, sometimes difficult.

In *non-coherent integration*, phase information is discarded. It works on real-valued data samples by adding up the magnitude (an envelope detector) or squared magnitude (*i.e.*, the power, a squared law detector) or sometimes log-magnitude of measurements. Because of the nonlinear operation, its analysis becomes more complicated. Squaring effectively removes phase variations from sample to sample (also unknown data bits if it exists) but it also squares the noise, allowing it to add up. Noncoherent integration is less efficient than coherent integration but it is often used when there are significant mismatches in signal phase due to Doppler frequency errors, unknown data modulation, and even receiver clock drifts.

Both coherent and non-coherent integrations schemes are well documented in textbooks and widely used in practical systems. A relatively new one is the semi-coherent integration scheme, which also has many other names. *Semi-coherent integration* can be defined as the sum of the products of the input signal with the conjugate of a delayed copy of itself. Since all conjugate products have a common phase argument (under constant frequency), they add "coherently." Each product contributing the signal's "power" to the sum, it is

therefore termed "semi-coherent." However, the delayed conjugate product operation also squares the noise, thus allowing it to add. It is less efficient than the coherent integration but slightly more efficient than the non-coherent integration in terms of integration loss and more robust against frequency variations.

In practical implementations, the coherent and non-coherent as well as semi-coherent integration schemes are typically used in combination. That is, a certain number of coherent integrations are followed by another number of non-coherent or semi-coherent integrations. The division of the total number of measurements into coherent and non-coherent or semi-coherent is a design parameter that needs to be trade-studied for a particular application at hand. This aspect is not covered in this paper. Another aspect that is not covered either is the post-detection integration (also called binary integration, "*M* out of *N*" detection, or classifier fusion). References can be found in [Richards, 2005; Kaplan and Hegarty, 2006].

When a single measurement is modeled as a constant signal A in a white zero-mean Gaussian noise with variance σ^2, the signal to noise ratio per measurement is defined as $(SNR)_1 = A^2/\sigma^2$ and it completely specifies the conditional pdfs and detection performance. When such N measurements are processed by coherent integration, the outcome is again a constant signal NA in a white zero-mean Gaussian noise with variance $N\sigma^2$. In this case, the output SNR easily can be calculated as $(SNR)_{CI} = NA^2/\sigma^2 = N(SNR)_1$. When compared to the single measurement SNR at the input, the output SNR is higher, proportional to the number of measurements integrated, thus achieving 100% efficiency. The ratio of the output SNR over the input SNR is called integration improvement factor in radar [Mahafza and Elsherbeni, 2004] or processing gain in GPS, denoted by G_{CI}, as:

$$G_{CI}(N) = \frac{(SNR)_{CI}}{(SNR)_1} = N \tag{1a}$$

$$G_{CI}(N)dB = 10\log_{10}\left(\frac{(SNR)_{CI}}{(SNR)_1}\right) = 10\log_{10}(N) \tag{1b}$$

For nonlinear integration schemes, however, the output SNR is not well defined. This is because with cross-product terms, it is difficult to properly separate signal from noise after such a nonlinear operation as squaring. As a result, with noise amplified by signal in the cross-product terms, nonlinear integration schemes are less effective and the resulting variance is signal-dependent.

There are two ways to quantify integration improvement for nonlinear integration schemes. One intuitive way is to define an equivalent SNR at the output of a nonlinear integration scheme such that the integration improvement factor can be calculated using the same formula as in Eq. (1). A rationale behind this approach is this. According to the central limit theorem, the sum of a large number of independent identical distributed (i.i.d.) samples converges to a Gaussian distribution with suitable mean and variance, which can be used to calculate the equivalent output SNR.

A more rigorous way, however, is to specify an equivalent SNR at the input (*i.e.*, a single measurement SNR) for a nonlinear integration scheme. The SNR required to achieve a specific P_d given a particular P_{fa} after N samples are integrated using the nonlinear integration scheme is denoted by $(SNR)_{NLI}$, which is smaller than $(SNR)_1$. They are related by:

$$(SNR)_{NLI} = (SNR)_1 \times G_{NLI}(N) \tag{2}$$

where $G_{NLI}(N)$ is the nonlinear integration improvement factor.

The nonlinear integration improvement factor $G_{NLI}(N)$ for a nonlinear integration scheme is typically smaller than the integration improvement factor $G_{CI}(N) = N$ for coherent integration. Their ratio is usually called the integration loss defined as:

$$L_{NLI} = G_{CI}(N)/G_{NLI}(N) = N/G_{NLI}(N) \tag{3}$$

Most of the results of integration schemes are available in the literature but scattered in different textbooks and research papers. In this paper, we compile them within a unified framework and present it in a cohesive and concise manner. We hope the paper can serve as an introductory material with key references listed for those who would like to study the subject further and a quick reference for those who would like to use it in their work.

The paper is organized as follows. We start with a review of the major results for detection of signal in noise with a single measurement. We then present coherent, non-coherent, and semi-coherent integration schemes as ways to combining multiple measurements, respectively. We next analyze results of comparative simulation study and finally conclude with a summary and future work.

REVIEW OF DETECTION THEORY WITH SINGLE MEASUREMENTS

Consider a complex measurement z consisting of a complex signal s and a complex noise w. We want to determine if the measurement z contains only noise w (denoted as the null hypothesis H_0) or both the desired signal s and noise w (denoted as the alternative hypothesis H_1):

$$H_0: \quad z = w \tag{4a}$$

$$H_1: \quad z = s + w \tag{4b}$$

The signal is modeled as $s = Ae^{j\theta}$ with A being a constant amplitude and θ a constant phase and the noise w is a complex white Gaussian noise with its real and imaginary components being of zero mean and variance σ^2.

The probability density functions (pdfs) that describe the measurement to be tested under each of the two hypotheses are denoted by $p(z|H_0)$ and $p(z|H_1)$, respectively. For an "optimal" choice between our two hypotheses, there are several criteria to choose. This includes the Neyman-Pearson criterion in which the decision is made to maximize the probability of detection P_d under the constraint that the probability of false alarm P_{fa} does not exceeds a predefined value, the Bayes minimum cost criterion, and maximization of the probability of a correct decision among others [Therrien, 1989; Kay, 1998]. The optimization under any of these criteria leads to the ubiquitous likelihood ratio test (LRT):

$$\Lambda(z) = \frac{p(z|H_1)}{p(z|H_0)} \underset{H_0}{\overset{H_1}{\gtrless}} \eta \tag{5a}$$

$$\ln\Lambda(z) = \ln\frac{p(z|H_1)}{p(z|H_0)} \underset{H_0}{\overset{H_1}{\gtrless}} \ln\eta \tag{5b}$$

$$\lambda(z) \underset{H_0}{\overset{H_1}{\gtrless}} T_d \tag{5c}$$

where η, $\ln\eta$ and T_d are detection thresholds for the corresponding formulations.

In Eq. (5a), $\Lambda(z)$ is the likelihood ratio test and in Eq. (5b), $\ln\Lambda(z)$ is called the log likelihood ratio test. The latter is computationally more efficient as most pdfs are in the form of exponentials and as a monotonic increasing operation, the taking of logarithm does not affect the detection performance (P_d and P_{fa}).

In Eq. (5c), $\lambda(z)$ is called the sufficient statistic, which, if it exists, is a function of the measurement z and has the property that the measurement z appears in the likelihood ratio or the log likelihood ratio only through $\lambda(z)$. In other words, knowing the sufficient statistic $\lambda(z)$ is as good as knowing the actual data z in making an optimal decision. As shown later in this paper, various integration schemes are such a sufficient statistic under different signal models.

The optimal detection problem now becomes solving for the detection threshold from equations of P_d and P_{fa} expressed in terms of the sufficient statistic $\lambda(z)$ and signal and noise model parameters. This typically involves two steps. A first step is to manipulate the conditional measurement pdfs, $p(z|H_0)$ and $p(z|H_1)$, so as to obtain the sufficient statistic pdfs, denoted by $p(\lambda|H_0)$ and $p(\lambda|H_1)$, respectively. A second step is to evaluate P_d and P_{fa} of the sufficient statistic as a function of the threshold T_d:

$$P_d = \int_{T_d}^{+\infty} p(\lambda|H_1)d\lambda \tag{6a}$$

$$P_{fa} = \int_{T_d}^{+\infty} p(\lambda|H_0)d\lambda \tag{6b}$$

Ideally, the threshold T_d can be "solved" from Eq. (6b) for a given level of false alarm P_{fa}. The probability of detection P_d is then calculated from Eq. (6a) as a function of the probability of false alarm P_{fa} with the threshold T_d as an intermediate. This P_d vs. P_{fa} relationship is the receiver operating characteristic (ROC) curve. Although the integrals can be expressed in terms of pdfs, there are typically no closed-form solutions except for simple cases. Numerical methods are popular means used to present the results in tables or plots.

From Eq. (4), the measurement pdf can be written as:

$$p(z) = \frac{1}{\pi\sigma^2}\exp\{\frac{-(z-s)^*(z-s)}{\sigma^2}\} \tag{7}$$

where the superscript * stands for complex conjugate. Under H_0, $s = 0$ and under H_1, $s \neq 0$. The log likelihood ratio is:

$$\ln\Lambda(z) = \frac{1}{\sigma^2}(2\mathrm{Re}\{s^*z\} - s^*s) \tag{8}$$

where $\mathrm{Re}\{z\}$ means the real part of z. Since the second term on the right hand side of Eq. (8) does not depend on the measurement, a sufficient statistic can be taken as:

$$\lambda(z) = \mathrm{Re}\{s^*z\} \tag{9}$$

Under H_1 with $s = A\exp(j\theta)$, Eq. (9) can be further written as:

$$\begin{aligned}\lambda(z) &= \mathrm{Re}\{s^*s + s^*w\} = A^2 + \mathrm{Re}\{wAe^{-j\theta}\} \\ &= E + \mathrm{Re}\{wAe^{-j\theta}\}\end{aligned} \tag{10}$$

where $E = A^2$ is the total energy in the expected signal s.

From Eq. (9), let $\zeta = s^*z$, which is a complex Gaussian. It is easy to show that under H_0, $\zeta \sim \mathcal{N}\{0, 2\sigma^2E\}$. Similarly, under H_1, $\zeta \sim \mathcal{N}\{E, 2\sigma^2E\}$. Since the power of the complex Gaussian noise splits evenly between the real and imaginary parts of ζ, it follows that the sufficient statistic $\lambda \sim \mathcal{N}\{0, \sigma^2E\}$ under H_0 and $\lambda \sim \mathcal{N}\{E, \sigma^2E\}$ under H_1. In other words, only half of the noise power competes with the signal energy in this case. The following equations can be established:

$$P_{fa} = \frac{1}{2}\left[1 - erf(\frac{T_d}{\sqrt{\sigma^2E}})\right] \tag{11a}$$

$$\begin{aligned}P_d &= \frac{1}{2}erfc\{erfc^{-1}(2P_{fa}) - \sqrt{\frac{E}{\sigma^2}}\} \\ &= \frac{1}{2}erfc\{erfc^{-1}(2P_{fa}) - \sqrt{(SNR)_1}\}\end{aligned} \tag{11b}$$

$$T_d = erf^{-1}(1-2P_{fa})\sqrt{\sigma^2E} \tag{11c}$$

where $(SNR)_1 = A^2/\sigma^2 = E/\sigma^2$ is the signal to noise ratio for a single measurement, erf(x) is the error function, and erfc(x) = 1 – erf(x) is the complementary error function defined as:

$$erf(x) = \frac{2}{\sqrt{\pi}} \int_0^x e^{-t^2} dt \tag{12a}$$

$$erfc(x) = \frac{2}{\sqrt{\pi}} \int_t^{+\infty} e^{-t^2} dt = 1 - erf(x) \tag{12b}$$

In the above derivations, it is implied that the signal s is perfectly known. However, it is merely the case in practice. It is rather more reasonable to assume that the initial phase is unknown and to model the signal as $s = \tilde{s} e^{j\theta}$ where the phase angle θ is a random variable uniformly distributed over [0, 2π) and independent of the signal components $\{\tilde{s}\}$. The pdf of H_0 is unchanged but that of H_1 now explicitly depends on θ, denoted by $p(z|\ H_1, \theta)$:

$$\begin{aligned} p(z \mid H_1, \theta) &= \frac{1}{\pi\sigma^2} \exp\{-\frac{(z - \tilde{s}e^{j\theta})^*(z - \tilde{s}e^{j\theta})}{\sigma^2}\} \\ &= \frac{1}{\pi\sigma^2} \exp\{-\frac{z^*z - 2|\tilde{s}^*z|\cos\theta + \tilde{s}^*\tilde{s}}{\sigma^2}\} \end{aligned} \tag{13}$$

Using the Bayesian rule for random parameters, the unconditional pdf $p(z|\ H_1)$ can be obtained by averaging the conditional pdf $p(z|\ H_1, \theta)$ over θ as:

$$\begin{aligned} p(z \mid H_1) &= \frac{1}{2\pi} \int_0^{2\pi} p(z \mid H_1, \theta) d\theta \\ &= \frac{1}{\pi\sigma^2} \exp\{-\frac{z^*z + \tilde{s}^*\tilde{s}}{\sigma^2}\} I_0(\frac{2|\tilde{s}^H z|}{\sigma^2}) \end{aligned} \tag{14}$$

where the last term $I_0(\cdot)$ is the modified Bessel function of the first kind (zero-order) defined as:

$$I_0(z) = \frac{1}{2\pi} \int_0^{2\pi} e^{z\cos(\theta)} d\theta$$

The log-LRT can be written as:

$$\ln \Lambda = \ln\left[I_0\left(\frac{2|\tilde{s}^H z|}{\sigma^2} \right) \right] \tag{15}$$

To avoid direct calculation of the Bessel function as well as the natural logarithm, it is desired to approximate $\ln[I_0(\cdot)]$ with a simple monotonically increasing function. It was shown in [Richards, 2005] that for small x, $\ln[I_0(x)] \approx x^2/4$ and for large x, $\ln[I_0(x)] \approx x$. In other words, the optimal detector is well approximated by a magnitude squaring operation or a square law detector for $x < 5$ dB whereas by an envelope detector when $x > 10$ dB. A practical sufficient statistic can thus be defined as:

Envelope Detector:

$$\lambda(z) = |\tilde{s}^* z| \underset{H_0}{\overset{H_1}{\gtrless}} T_d, \quad |\tilde{s}^* z| > 10 \text{ dB} \tag{16a}$$

Square Law Detector:

$$\lambda(z) = |\tilde{s}^* z|^2 \underset{H_0}{\overset{H_1}{\gtrless}} T_d, \quad |\tilde{s}^* z| < 5 \text{ dB} \tag{16b}$$

The performance of the envelope detector specified in Eq. (16a) can be established by noting that $\tilde{s}^* z \sim \mathcal{N}\{0, 2\sigma^2 E\}$ under H_0 and $\sim \mathcal{N}\{A^2, 2\sigma^2 E\}$ under H_1. Then, under H_0, $\lambda = |\tilde{s}^* z|$ is Rayleigh distributed:

$$p(\lambda \mid H_0) = \begin{cases} \frac{\lambda}{E\sigma^2} \exp\left(-\frac{\lambda^2}{2E\sigma^2} \right) & \lambda \geq 0 \\ 0 & \lambda < 0 \end{cases} \tag{17}$$

And under H_1, λ is Rician distributed:

$$p(\lambda \mid H_1) = \begin{cases} \frac{\lambda}{E\sigma^2} \exp\left(-\frac{\lambda^2 + E^2}{2E\sigma^2} \right) I_0(\frac{\lambda}{\sigma^2}) & \lambda \geq 0 \\ 0 & \lambda < 0 \end{cases} \tag{18}$$

From Eq. (17), the probability of false alarm can be calculated as:

$$P_{fa}(\lambda \mid H_0) = \int_{T_d}^{+\infty} p(\lambda \mid H_0) d\lambda = \exp\left(\frac{-T_d^2}{E\sigma^2} \right) \tag{19}$$

Inverting this equation gives the detection threshold as:

$$T_d = \sqrt{-E\sigma^2 \ln P_{fa}} \tag{20}$$

From Eq. (18), the probability of detection can be calculated, with the threshold from Eq. (18), as:

$$\begin{aligned} P_d(\lambda \mid H_1) &= Q_M\left(\sqrt{\frac{E}{\sigma^2}}, \sqrt{\frac{T_d^2}{E\sigma^2}} \right) \\ &= Q_M(\sqrt{(SNR)_1}, \sqrt{-\ln P_{fa}}) \end{aligned} \tag{21a}$$

where $Q_M(\cdot, \cdot)$ is the Marcum's Q function defined as:

$$Q_M(\alpha, \tau) = \int_{\tau}^{+\infty} t \exp\left[-\tfrac{1}{2}(t^2 + \alpha^2) \right] I_0(\alpha t) dt \tag{21b}$$

Compared to the coherent detector given in Eq. (9), the envelope detector requires higher SNR to achieve the same performance. This extra SNR required to maintain the same detection performance is called the detector loss, a price paid for not knowing the signal phase. With $P_{fa} = 10^{-6}$, the envelope detector requires 0.6 dB higher SNR than the coherent detector to achieve $P_d = 0.9$ and about 0.7 dB more at $P_d = 0.5$.

Instead of averaging the H_1's pdf over unknown parameters to obtain an unconditional pdf as in Eq. (14), another approach is to use the generalized likelihood ratio test (GLRT), in which the likelihood ratio is expressed as a function of the unknown signal parameter. In addition to averaging the GLRT over the region of the unknown parameter, which may be assumed uniformly distributed

if there is no better model available, another approach is to obtain an estimate of the parameter by maximizing the likelihood ratio over the unknown parameter and then to compare the maximized likelihood ratio to the threshold for detection. The maximization can be done analytically or numerically and the latter is the theoretic basis for parametric search (sequential or parallel) in detection.

Another signal parameter that is usually unknown is the signal amplitude A, which is assumed to be a deterministic scale factor. Eqs. (11b) and (21a) do not depend explicitly on A (or the noise power σ^2) but rather on their ratio $(SNR)_1$ for evaluating the detection performance. However, a practical implementation requires specific values to set up the detection threshold. One is to use a reference signal with unit energy $\hat{s}$ such that $s = \tilde{s}e^{j\theta} = A\hat{s}e^{j\theta}$. For weak signals, another approach is to implement a locally optimum detector (LOD) for unknown A, which maximizes the slope of the likelihood ratio at $A = 0$ while keeping a fixed P_{fa} [Kassam, 1988].

COHERENT INTEGRATION – OPTIMAL COMBINING OF MULTIPLE MEASUREMENTS

After introducing the signal model, this section first formulates the perfect case with known signal. It then presents the formulation with unknown signal phase. Direct summation is then presented followed by the use of FFT as an approach to coherent integration.

Signal Model

Consider N measurements where each measurement z_n, made at time index n, has the following model:

$$z_n = s_n + w_n, \quad n = 0, \ldots, N\text{-}1 \tag{22}$$

where s_n is the signal and w_n is a complex white Gaussian noise with $\mathrm{Re}\{w_n\} \sim \mathcal{N}(0, \sigma^2)$ and $\mathrm{Im}\{w_n\} \sim \mathcal{N}(0, \sigma^2)$. Putting the N measurements into a vector format gives:

$$\underline{z} = [z_0, \quad \cdots, \quad z_{N-1}]^T \tag{23a}$$

$$\underline{s} = [s_0, \quad \cdots, \quad s_{N-1}]^T \tag{23b}$$

$$\underline{w} = [w_0, \quad \cdots, \quad w_{N-1}]^T \tag{23c}$$

The joint pdf for N complex measurement samples is:

$$p(\underline{z}) = \frac{1}{\pi^N \sigma^{2N}} \exp\{\frac{-(\underline{z}-\underline{s})^H(\underline{z}-\underline{s})}{\sigma^2}\} \tag{24}$$

where H is the Hermitian (conjugate transpose) operator.

General Formulation for Perfect Signal Model

The log likelihood ratio is:

$$\ln \Lambda(\underline{z}) = \frac{1}{\sigma^2}(2\,\mathrm{Re}\{\underline{s}^H \underline{z}\} - \underline{s}^H \underline{s}) \tag{25}$$

A sufficient statistic can be defined as:

$$\lambda(\underline{z}) = \mathrm{Re}\{\underline{s}^H \underline{z}\} \tag{26}$$

From Eq. (26), it can be seen that the LRT leads to a rather simple sufficient statistic, which specifies the data processing to be performed on the measurements. It affords several interpretations [Richards, 2005]. The term $\underline{s}^H\underline{z}$ is a dot product of the complex vectors $\underline{s}$ and $\underline{z}$. It can be viewed as a correlation operation. This dot product represents an FIR filtering operation, evaluated at the particular instant when the equivalent finite impulse response $\underline{s}$ completely overlaps with the data vector $\underline{z}$. It can also be viewed as a *matched filter*, thus detecting the presence of the mean vector in the data.

Under H_1 with $s_n = A_n \exp(j\phi_n)$, Eq. (26) can be further written as:

$$\lambda(\underline{z}) = \mathrm{Re}\{\underline{s}^H \underline{s} + \underline{s}^H \underline{w}\} = \mathrm{Re}\{\sum_{n=0}^{N-1} |A_n|^2 + \sum_{n=0}^{N-1} w_n A_n e^{-j\phi_n}\}$$
$$= E + \mathrm{Re}\{\sum_{n=0}^{N-1} w_n A_n e^{-j\phi_n}\} \tag{27}$$

where $E = \sum_{n=0}^{N-1} |A_n|^2$ is the total energy in the expected signal $\underline{s}$ and $E = NA^2$ in the equal mean case with $A_n = A$.

Let $\zeta = \underline{s}^H\underline{z}$, which is a complex Gaussian because it is a sum of Gaussian random variables. It is easy to show that under H_0, $\zeta \sim \mathcal{N}\{0, 2\sigma^2 E\}$. Similarly, under H_1, $\zeta \sim \mathcal{N}\{E, 2\sigma^2 E\}$. The sufficient statistic $\lambda \sim \mathcal{N}\{0, \sigma^2 E\}$ under H_0 and $\lambda \sim \mathcal{N}\{E, \sigma^2 E\}$ under H_1. Eqs. (11a), (11b), and (11c) for the probability of false alarm, probability of detection, and detection threshold respectively, are directly applicable.

Eq. (26) is called a coherent detector since it assumes the perfect knowledge of the signal $\underline{s}$. From Eq. (26) or Eq. (27), the signal power after the operation (a dot product) is A^2N^2 whereas the noise variance is $N\sigma_w^2$. The SNR at the coherent detector's output, denoted by $(SNR)_{CD}$, is then related to $(SNR)_1$ by:

$$(SNR)_{CD} = \frac{E^2}{\sigma^2 E} = \frac{E}{\sigma^2} = \frac{NA^2}{\sigma^2} = N(SNR)_1 \tag{28}$$

This improves the single measurement SNR by a factor of N.

General Formulation with Unknown Phase

In practice, however, the signal $\underline{s}$ is not perfectly known. Assume that the initial phase is unknown and the signal can be written as $\underline{s} = \tilde{\underline{s}}e^{j\theta}$ where the phase angle θ is a random variable uniformly distributed over $[0, 2\pi)$ and independent of the signal components $\{\tilde{s}_n\}$. The pdf of H_0 is unchanged but that of H_1 now explicitly depends on θ, denoted by $p(\underline{z}|\, H_1, \theta)$:

$$p(\underline{z} \mid H_1, \theta) = \frac{1}{\pi^N \sigma^{2N}} \exp\{-\frac{1}{\sigma^2}(\underline{z} - \tilde{\underline{s}}e^{j\theta})^H(\underline{z} - \tilde{\underline{s}}e^{j\theta})\}$$

$$= \frac{1}{\pi^N \sigma^{2N}} \exp\{-\frac{1}{\sigma^2}(\underline{z}^H \underline{z} - 2|\underline{\tilde{s}}^H \underline{z}| \cos\theta + \underline{\tilde{s}}^H \underline{\tilde{s}})\} \quad (29)$$

which can be averaged over θ, leading to the unconditional pdf $p(\underline{y}|\, H_1)$:

$$p(\underline{z}\,|\,H_1) = \frac{1}{2\pi}\int_0^{2\pi} p(\underline{z}\,|\,H_1,\theta)d\theta$$

$$= \frac{1}{\pi^N \sigma^{2N}} \exp\{-(\frac{1}{\sigma^2}\underline{z}^H \underline{z} + \underline{\tilde{s}}^H \underline{\tilde{s}})\} I_0(\frac{2|\underline{\tilde{s}}^H \underline{z}|}{\sigma^2}) \quad (30)$$

The log-LRT is:

$$\ln\Lambda = \ln\left[I_0\left(\frac{2|\underline{\tilde{s}}^H \underline{z}|}{\sigma^2}\right)\right] \quad (31)$$

Similar to Eqs. (16a) and (16b), the same approximations can be used to obtain the sufficient statistic as:

Envelope Detector: $\lambda(\underline{z}) = |\underline{\tilde{s}}^H \underline{z}| \underset{H_0}{\overset{H_1}{\gtrless}} T_d$ (32a)

Square Law Detector: $\lambda(\underline{z}) = |\underline{\tilde{s}}^H \underline{z}|^2 \underset{H_0}{\overset{H_1}{\gtrless}} T_d$ (32b)

The performance of the envelope detector specified in Eq. (32a) can be established by noting that $\underline{\tilde{s}}^H \underline{z} \sim \mathcal{N}\{0, 2\sigma^2 E\}$ under H_0 and $\sim \mathcal{N}\{E, 2\sigma^2 E\}$ under H_1 where E is the total energy in $\underline{\tilde{s}}$. Then, $\lambda = |\underline{\tilde{s}}^H \underline{z}|$ follows a Rayleigh distribution under H_0 as given in Eq. (17) and a Rician distribution under H_1 as given in Eq. (18). Similarly, Eqs. (19), (20), and (21a) for the probability of false alarm, detection threshold, and probability of detection, respectively, are directly applicable [Skolnik, 2001].

Direct Summation for Constant Signal

In the above analysis, the detection of a signal in noise is treated as a likelihood ratio test. The formulation of joint detection with multiple measurements leads to the structure of coherent integration (a dot product/a matched filter/a correlator/an finite impulse response (FIR) filter) followed by detection. A coherent detector is used when the signal model is perfectly known whereas an envelope detector or a square law detector is used when the initial phase of the signal is not known. In the following, we discuss two practical implementations of coherent integration. They are (1) direct summation and (2) coherent integration with the fast Fourier transform (FFT).

With the noise characteristics known, it is the signal model (*i.e.*, its structure and parameters and our knowledge of it) that determines the solution of optimal detection. When the signal is constant, the direct summation of N measurements is given by:

$$\zeta_{DS} = \sum_{n=0}^{N-1} z_n = \underline{1}_N{}^T \underline{z} = \sum_{n=0}^{N-1} s_n + \sum_{n=0}^{N-1} w_n \quad (33)$$

where $\underline{1}_N$ is an $N\times 1$ vector of all ones.

From the above analysis, it is clear that $\lambda(\underline{z}) = \mathrm{Re}\{\zeta_{DS}\}$ is the optimal detector for the case where $s_n = A$. The signal amplitude A does not appear in the detector but rather a reference signal of unit is used instead. When the phase θ is unknown, the optimal detector can be either $\lambda(\underline{z}) = |\zeta_{DS}|$ or $\lambda(\underline{z}) = |\zeta_{DS}|^2$ depending on the magnitude of the sum.

For the optimal detector in Eq. (33) based on the model of a constant signal, we are now to analyze its behavior when the signal is actually a sine wave with a constant frequency f_d. Under this condition, Eq. (33) can be written as:

$$\zeta_{DS} = A\exp\{j\pi f_d T_s(N-1)\}\frac{\sin(\pi f_d T_s N)}{\sin(\pi f_d T_s)} + \sum_{n=0}^{N-1} w_n$$

$$= A\exp\{j\pi f_d T_s(N-1)\}\frac{\sin(\pi f_d T_s N)}{\pi f_d T_s N} / \frac{\sin(\pi f_d T_s)}{\pi f_d T_s} N$$

$$+ \sum_{n=0}^{N-1} w_n \quad (34)$$

When the Doppler frequency is small, $f_d T_s N \sim 0$ and $sinc(\pi f_d T_s N) = sin(\pi f_d T_s N)/\pi f_d T_s N \sim 1$. The direct sum can be simplified into

$$\zeta_{DS} \approx \exp\{j\pi f_d T_s(N-1)\} AN + \sum_{n=0}^{N-1} w_n \approx AN + \sum_{n=0}^{N-1} w_n \quad (35)$$

The signal power after the direct sum (only consider the real component) is A^2N^2 whereas the noise variance is $N\sigma^2$. The direct sum's SNR, denoted by $(SNR)_{DS}$, is then given by $(SNR)_{DS} = A^2N^2/N\sigma^2 = NA^2/\sigma^2 = N(\mathrm{SNR})_1$. It improves the input SNR by a factor of N. However, when the Doppler frequency is large, the SNR improvement vanishes rather quickly in the form of a *sinc*-function.

Coherent Integration with FFT

For a signal with a constant Doppler frequency, the LRT can be first averaged over the unknown initial phase and then expressed as a function of the unknown frequency f_d. Averaging again over f_d within the unambiguous interval from 0 to $1/T_s$ (or $-1/2T_s$ to $1/2T_s$) leads to the following sufficient statistic:

$$\zeta_{CI}(\underline{z}) = \int_0^{1/T_s} I_0(2|\underline{z}^H \underline{\tilde{s}}(f)|)df \quad (36a)$$

where $\underline{\tilde{s}}$ is a signal replica defined as:

$$\underline{\tilde{s}}(f) = [\tilde{s}_0(f), \quad \cdots, \quad \tilde{s}_{N-1}(f)]^T \quad (36b)$$

$$\tilde{s}_n(f_k) = \exp\{j2\pi f_k T_s n\} \quad (36c)$$

with f_k being a test frequency (which also differs from the true signal $\underline{s}$ in amplitude and initial phase).

For practical implementation, the integral in Eq. (36a) is replaced with a filter bank with N filters as:

$$\zeta_{CI}(\underline{z}) = \frac{1}{N}\sum_{k=0}^{N-1} I_0(2\,|\,\underline{z}^H \underline{\tilde{s}}(f_k)\,|), \quad \text{with } f_k = \frac{k}{NT_s},\ k = 0, \ldots, N\text{-}1 \qquad (37)$$

The test function can be approximated by the following sufficient statistic:

$$\lambda_{CI}(\underline{z}) \approx \max_k |\, z_{CI}(f_k)\,| \approx \max_k |\, \underline{\tilde{s}}(f_k)^H \underline{z}\,| \qquad (38)$$

The coherent sum in Eq. (38) can be viewed as successive rotation of the phase of measurements by an amount specified by the signal replica so as to align the measurements to the same phase prior to summation. It in fact implements a matched filter with a filter parameter f_k. Since the frequency is unknown, it is searched over a range of possible values either in parallel or in sequence.

When the filter parameter is discretized into a set of N parameters with a frequency spacing inversely proportional to the signal interval, *i.e.*, $f_k = k/NT_s$, $k = 0, \ldots, N\text{-}1$, it represents a conventional filter bank, which can be realized with FFT. For the filter in which $f_k \approx f_d$, its output is close to Eq. (32) with a SNR increased by a factor of proportional to N.

NON-COHERENT INTEGRATION SCHEMES

The amplitude and phase of a signal to be detected are typically unknown. Ignoring the amplitude in the LRT does not affect the detection performance and a reference signal of unit amplitude is typically used. The unknown phase can be averaged out from the conditional pdf or from the LRT, leading to an envelope detector or a square law detector as in Eq. (32). Intuitively, taking magnitude (or squared magnitude or log-magnitude) effectively removes the unknown phase (as well as phase modulation if it exists on the signal). After the phase information is discarded, combining magnitude samples is referred as non-coherent integration, which is analyzed below.

The measurement model in Eq. (22) can be expressed in terms of its real and imaginary parts or equivalently in magnitude and phase as:

$$z_n = s_n + w_n = \xi_n + j\eta_n = r_n \exp\{j\varphi_n\} \qquad (39a)$$

where

$$\xi_n = \mathrm{Re}\{s_n + w_n\} = r_n \cos(\varphi_n) \qquad (39b)$$

$$\eta_n = \mathrm{Im}\{s_n + w_n\} = r_n \sin(\varphi_n) \qquad (39c)$$

$$r_n = |z_n| = \sqrt{(\mathrm{Re}\{s_n + w_n\})^2 + (\mathrm{Im}\{s_n + w_n\})^2} \qquad (39d)$$

$$\varphi_n = \tan^{-1}(\mathrm{Im}\{s_n + w_n\} / \mathrm{Re}\{s_n + w_n\}) \qquad (39e)$$

$$r_n^2 = z_n^* z_n = \xi_n^2 + \eta_n^2 \qquad (39f)$$

The joint pdf for r and φ is given by:

$$p(r,\varphi) = \frac{r}{2\pi\sigma^2}\exp\{-\frac{r^2 + A^2}{2\sigma^2}\}\exp\{\frac{rA\cos(\varphi)}{\sigma^2}\} \qquad (40)$$

The pdf for r alone is obtained by integrating Eq. (40) over φ, yielding:

$$p(r) = \int_0^{2\pi} p(r,\varphi)d\varphi = \frac{r}{\sigma^2}\exp\{-\frac{r^2 + A^2}{2\sigma^2}\} I_0(\frac{rA}{\sigma^2}) \qquad (41)$$

Similarly, the pdf for φ alone can be obtained by integrating Eq. (40) over r.

Under H_0, $A = 0$ (noise alone), Eq. (40) becomes the Rayleigh probability density function:

$$p(r) = \frac{r}{\sigma^2}\exp\{-\frac{r^2}{2\sigma^2}\} \qquad (42a)$$

$$p(\varphi) = \frac{1}{2\pi},\ \varphi \in (0,\quad 2\pi) \qquad (42b)$$

Under H_1, $A \neq 0$, Eq. (41) is the Rician probability density function. Also when A/σ^2 is very large, Eq. (41) becomes a Gaussian probability density function with mean A and variance σ^2.

Let $\underline{r} = [r_0, \ldots, r_{N-1}]^T$ be a vector of N magnitude samples. The joint pdfs under H_0 and H_1 are

$$p(\underline{r}\,|\,H_0) = \prod_{n=0}^{N-1}\frac{r_n}{\sigma^2}\exp\{-\frac{r_n^2}{2\sigma^2}\} \qquad (43a)$$

$$p(\underline{r}\,|\,H_1) = \prod_{n=0}^{N-1}\frac{r_n}{\sigma^2}\exp\{-\frac{r_n^2 + A^2}{2\sigma^2}\} I_0(\frac{r_n A}{\sigma^2}) \qquad (43b)$$

With the same approximation as used to derive Eq. (32b) or (16b), the log-LRT becomes

$$\ln\Lambda = \sum_{n=0}^{N-1}\ln\left[I_0(\frac{r_n A}{\sigma^2})\right] \approx \sum_{n=0}^{N-1}\frac{r_n^2 A^2}{\sigma^4} \qquad (44)$$

Combining all constants into the threshold leads to a practical sufficient statistic as:

$$\lambda = \sum_{n=0}^{N-1} r_n^2 = \sum_{n=0}^{N-1} |\, z_n\,|^2 \underset{H_0}{\overset{H_1}{\gtrless}} T_d \qquad (45)$$

which specifies a noncoherent integration detection rule using the square law detector. A similar noncoherent integration detection rule using the envelope detector can result if the log-LRT is approximated using Eq. (32a) or (16a).

To determine the detection performance, we start with calculating the pdfs for the sufficient statistic in Eq. (45). First, let $q = r^2$ and we determine the pdfs for q from Eq. (43) as:

$$p(q) = \frac{1}{2\sigma^2}\exp\{-\frac{q + A^2}{2\sigma^2}\} I_0(\frac{\sqrt{q}A}{\sigma^2}) \qquad (46)$$

When $A = 0$, $q = r^2 = \xi^2 + \eta^2$ obeys the Chi-square (χ^2) distribution with two degrees of freedom, which is also an exponential distribution. For $A \neq 0$, it obeys a non-central Chi-square (χ^2) distribution. When the degrees of freedom exceed 30, a non-central Chi-square (χ^2) distribution can be accurately approximated by a Gaussian distribution.

Since the random variables r_n (and the corresponding $q_n = r_n^2$) for all n are independent, the pdf for the sufficient statistic λ can be derived as the convolution of individual pdfs:

$$p(\lambda \mid H_1) = \left(\frac{\lambda}{4N\sigma^2(SNR)_1}\right)^{\frac{N-1}{2}} \exp\{-\frac{\lambda}{4\sigma^2} - N(SNR)_1\} \times I_{N-1}\left(\sqrt{\frac{N(SNR)_1\lambda}{\sigma^2}}\right) \quad (47)$$

where $(SNR)_1 = A^2/\sigma^2$ as previously defined and $I_{N-1}(\cdot)$ is the modified Bessel function of order N-1.

When $A = 0$, the pdf for the sufficient statistic λ is χ^2–distributed with $2N$ degrees of freedom, which can be written as:

$$p(\lambda \mid H_0) = \frac{1}{\sigma^{2N} 2^N \Gamma(N)} \lambda^{N-1} \exp\{-\frac{\lambda}{2\sigma^2}\} \quad (48)$$

where $\Gamma(N) = (N\text{-}1)!$ is the Gamma function. As a special case of the gamma density, the Erlang density reduces to the exponential pdf when $N = 1$.

The probability of false alarm is obtained by integrating the pdf in Eq. (48) from the threshold to infinity as:

$$P_{fa}(\lambda \mid H_0) = \int_{T_d}^{+\infty} p(\lambda \mid H_0) d\lambda = 1 - I\left(\frac{T_d}{\sqrt{N}}, N-1\right) \quad (49)$$

where the last term is called Pearson's form of the incomplete gamma function defined as

$$I(u, M) = \int_0^{u\sqrt{M+1}} \frac{e^{-\tau}\tau^M}{M!} d\tau \quad (50)$$

The probability of detection is obtained by integrating the pdf in Eq. (47) from the threshold to infinity as:

$$P_d(\lambda \mid H_1) = \int_{T_d}^{+\infty} p(\lambda \mid H_0) d\lambda = Q_M\left(\sqrt{\frac{2NA^2}{\sigma^2}}, \sqrt{2T_d}\right) + e^{-(T + \frac{NA^2}{\sigma^2})} \sum_{m=2}^{N} \left(\frac{T_d\sigma^2}{NA^2}\right)^{\frac{m-1}{2}} I_{m-1}\left(2\sqrt{\frac{NT_dA^2}{\sigma^2}}\right) \quad (51)$$

Closed-form solutions generally do not exist for these integrals. Numerical solutions are often used to generate tables and curves. However, some empirical approximations exist for manual calculation. One example is Albersheim's equations [Richards, 2005].

Non-coherent integration is less efficient than coherent integration. The non-coherent integration gain is always smaller than that of the coherent integration for the same number of measurements. This integration loss, estimated somewhere between $\sqrt{N}$ and N, is approximated by a simple formula [DiFranco and Rubin, 1980]:

$$L_{NCI} = 10\log(\sqrt{N}) - 5.5, \text{ dB} \quad (52)$$

Another approximation for the integration loss factor [Barton, 1988; Curry, 2001] is:

$$L_{NCI} = \frac{1 + (SNR)_1}{(SNR)_1} \quad (53)$$

Yet another approximation, which is accurate within 0.8 dB given by [Peebles, 1998], is in terms of integration improvement factor as:

$$G(N)_{NCI} = 6.79(1 + 0.235P_d)\left(1 + \frac{\log_{10}(1/P_{fa})}{46.6}\right)\log_{10}(N) \times [1 - 0.14\log_{10}(N) + 0.01831\log_{10}^2(N)], \text{ dB} \quad (54)$$

Using Eq. (53), the output SNR after non-coherent integration can be written as:

$$(SNR)_{NCI} = \frac{(SNR)_{CI}}{L_{NCI}} = \frac{N(SNR)_1}{L_{NCI}} = N(SNR)_1 \frac{(SNR)_1}{1 + (SNR)_1} \quad (55)$$

Strictly speaking, the integration loss factor or improvement factor ought to be specified by calculating an equivalent SNR at the input (*i.e.*, a single measurement SNR) that is required to achieve a specific P_d given a particular P_{fa} after N samples are integrated using a nonlinear integration scheme. This is because the output SNR for a nonlinear integration scheme is not well defined due to cross-product terms.

However, some equivalent SNR is frequently used at the output of a nonlinear integration scheme. One definition is given in [Kay, 1998] as:

$$(SNR)_{LNI} = \frac{E\{z \mid H_1\} - E\{z \mid H_0\}}{\sqrt{Var\{z \mid H_0\}}} \quad (56)$$

where the square root is used for variance in the denominator so that the output SNR is the ratio of the same units as the input SNR.

As another example, consider the non-coherent integration scheme using an energy detector in Eq. (45). It is easy to show that

$$E\{\lambda \mid H_0\} = 2N\sigma^2 \quad (57a)$$

$$Var\{\lambda \mid H_0\} = 8N\sigma^4 \quad (57b)$$

$$E\{\lambda \mid H_1\} = N(A^2 + 2\sigma^2) \quad (57c)$$

According to Eq. (56), the SNR for the sufficient statistic in Eq. (45) is:

$$(SNR)_{NCI\_ED} = \frac{A^2}{2\sigma^2}\sqrt{\frac{N}{2}} = \sqrt{\frac{N}{2}}(SNR)_1 \tag{58}$$

Compared to coherent integration, the corresponding integration loss is:

$$L_{NCI\_ED} = \sqrt{2N} \approx 1.4\sqrt{N} \tag{59}$$

which is consistent with the loss estimates given before.

Consider yet another example where the integration is done of N outputs from an envelope detector as:

$$\lambda = \sum_{n=0}^{N-1} r_n = \sum_{n=0}^{N-1} |z_n| \underset{H_0}{\overset{H_1}{\gtrless}} T_d \tag{60}$$

which can be viewed as if the log-LRT Eq. (44) is approximated using Eq. (32a). The envelope detector's output follows a Rayleigh distribution Eq. (42a) under H_0 and a Ricean distribution Eq. (41) under H_1, respectively. The conditional means and variances can be computed as:

$$E\{r \mid H_0\} = \sqrt{\frac{\pi}{2}}\sigma \tag{61a}$$

$$Var\{r \mid H_0\} = E\{r^2 \mid H_0\} - E^2\{r \mid H_0\} = \frac{4-\pi}{2}\sigma^2 \tag{61b}$$

$$E\{r \mid H_1\} = \sqrt{\frac{\pi}{2}}\sigma e^{-\frac{A^2}{4\sigma^2}}\left[(1+\frac{A^2}{2\sigma^2})I_0(\frac{A^2}{2\sigma^2}) + \frac{A^2}{2\sigma^2}I_1(\frac{A^2}{4\sigma^2})\right] \tag{61c}$$

$$Var\{r \mid H_1\} = A^2 + 2\sigma^2 - E^2\{r \mid H_1\} \tag{61d}$$

Both Eqs. (61a) and (61b) can be derived from Eqs. (61c) and (61d) by setting $A = 0$. Assume that $\{r_n\}$ are i.i.d. and then the conditional means and variances of λ can be computed from those of r_n in Eqs. (61a) through (61d) as:

$$E\{\lambda \mid H_0\} = NE\{r \mid H_0\} = N\sqrt{\frac{\pi}{2}}\sigma \tag{62a}$$

$$Var\{\lambda \mid H_0\} = NVar\{r \mid H_0\} = N\frac{4-\pi}{2}\sigma^2 \tag{62b}$$

$$E\{\lambda \mid H_1\} = NE\{r \mid H_1\} = N\sqrt{\frac{\pi}{2}}\sigma e^{-\frac{A^2}{4\sigma^2}} \times \left[(1+\frac{A^2}{2\sigma^2})I_0(\frac{A^2}{2\sigma^2}) + \frac{A^2}{2\sigma^2}I_1(\frac{A^2}{4\sigma^2})\right] \tag{62c}$$

$$Var\{\lambda \mid H_1\} = NVar\{r \mid H_1\} = N(A^2 + 2\sigma^2 - E^2\{r \mid H_1\}) \tag{62d}$$

The output SNR of non-coherent integration with an envelope detector according to Eq. (60) is:

$$(SNR)_{NCI\_ED} = \sqrt{N}\sqrt{\frac{\pi}{4-\pi}}\left(e^{-\frac{A^2}{4\sigma^2}}\left[(1+\frac{A^2}{2\sigma^2})I_0(\frac{A^2}{2\sigma^2}) + \frac{A^2}{2\sigma^2}I_1(\frac{A^2}{4\sigma^2})\right] - 1\right)$$
$$= \sqrt{N}\sqrt{\frac{\pi}{4-\pi}}\left(e^{-\frac{(SNR)_1}{4}}\left[(1+\frac{(SNR)_1}{2})I_0(\frac{(SNR)_1}{2}) + \frac{(SNR)_1}{2}I_1(\frac{(SNR)_1}{4})\right] - 1\right) \tag{63}$$

The following approximations are given by [Lowe, 1999]:

$$(SNR)_{NCI\_ED} \approx \sqrt{N}\sqrt{\frac{\pi}{4-\pi}}\left(\frac{(SNR)_1}{4} - \frac{(SNR)_1^2}{64} + \frac{(SNR)_1^3}{768}\right), \quad (SNR)_1 \le 2.8 \tag{64a}$$

$$(SNR)_{NCI\_ED} \approx \sqrt{N}\sqrt{\frac{2}{4-\pi}}\left(\sqrt{(SNR)_1} - \sqrt{\frac{\pi}{2}} + \frac{1}{2(SNR)_1} + \frac{1}{8(SNR)_1^{3/2}} + \frac{3}{16(SNR)_1^{5/2}}\right), \quad (SNR)_1 \ge 2.8 \tag{64b}$$

When $(SNR)_1 \ll 1$, the signal is too weak to detect from a single measurement. The lower order term in Eq. (64a) indicates that the output SNR is proportional to $(SNR)_1$ but to the square root of N at this regime. From Eq. (64a), the loss can be written as:

$$L_{NCI\_ED} \approx \sqrt{\frac{4(4-\pi)}{\pi}N} \approx 1.05\sqrt{N} \tag{65}$$

Other effects that further introduce SNR loss include amplitude fluctuations such as Swerling models [Richards, 2005] and phase noise [Richards, 2003], which are not covered in this paper.

SEMI-COHERENT INTEGRATION SCHEMES

For a signal $\underline{z}$ of length N with an amplitude A, there are an unknown initial phase ϕ_0 and an unknown Doppler frequency f_d. The initial unknown phase can be averaged out as done previously. The resulting likelihood ratio can be further averaged over the phase increment caused by the unknown Doppler per sampling interval, denoted by $\varphi = 2\pi f_d T_s$ (the total phase is $\phi_n = \phi_0 + \varphi n$), which may be assumed uniformly distributed over $[0, 2\pi)$. The log-LRT can be written as:

$$Ln\Lambda = \frac{1}{2\pi}\int_0^{2\pi} I_0(2A|\underline{z}^H \underline{\tilde{s}}(\varphi)|)d\varphi \tag{66}$$

The Bessel function $I_0(\blacksquare)$ in Eq. (66) can be approximated by a Taylor series for small values of A. According to [Selin, 1965], the result is:

$$Ln\Lambda = \frac{A^2}{64}\left[\frac{16}{A^2}S_0 + S_0^2 + 2\sum_{k=1}^{N}|S_k|^2\right] \tag{67}$$

where

$$S_k = \sum_{n=k+1}^{N} z_n z_{n-k}^* \tag{68}$$

The only term in Eq. (67) that depends on the signal's Doppler phase is the sum with S_k for $k \neq 0$ whereas the other two terms involve the total power S_0 from both the signal and noise. It was suggested in [Wirth, 2001] to use the sum with S_k in Eq. (68) as a test function:

$$T_K = \sum_{k=1}^{K}|S_k|^2 \tag{69}$$

which is also called the autocorrelation estimate (ACE) test because S_k is related to the ACE of the signal series $\{z_n\}$ for the time lag kT_s by:

$$\rho_k = \frac{1}{N-k}\sum_{n=k+1}^{N} z_n z_{n-k}^* = \frac{1}{N-k} S_k \tag{70}$$

The parameter K is at most N-1. When $K = 0$, we have $k = 0$ and $T_0 = S_0$. This corresponds to non-coherent integration (with a square law detector or by power-combination) discussed in the previous section. $K = 1$ leads to $k = 1$, which corresponds to the so-called tone detector to be discussed later. In general, the detection performance improves with increasing K. However, with a large k, the number of samples available for calculating S_k is reduced. Typically, $K/N = ¼ \sim ½$.

For a signal with constant Doppler $z_n = A\exp(j\varphi n)$, the product of the input signal with the conjugate of a delayed copy of itself, *i.e.*, $z_n z_{n-k}^* = A^2 \exp(j\varphi k)$, has a phase argument independent of n. As a result, the summation in Eq. (68) adds $z_n z_{n-k}^*$ "coherently" for all the measurement contributions over n. But what each measurement contributes to the sum is the signal "power." It is in this sense that the summation is called "semi-coherent." Delayed squaring, although removing phase variations from sample to sample (and also unknown data bits), also squares the noise, thus allowing it to add up. It is therefore less effective than coherent integration.

For a small k, an additional SNR is required to achieve the same detection performance as an ideal coherent integration, which is the integration loss mentioned earlier. As noted in [Wirth, 2001], the ACE test is expected to operate on a single signal and a weak signal may be suppressed by a stronger signal due to the nonlinear nature of the test. It was shown in [Wirth, 2001] that for $K = N/2$, the loss compared to a filter bank is only 0.5 dB. Since a filter bank may suffer from a straddling loss about 1 dB, there may even be a gain of 0.5 dB compared to a filter bank. Another advantage of the ACE test is that it is more robust against frequency variations. In the next section, we will show these results via computer simulations.

Now consider the special case where $K = 1$. The summation of $z_n z_{n-k}^*$ over n for $k = 1$ is:

$$\zeta = \sum_{n=0}^{N-2} \kappa_n z_{n+1} z_n^* \tag{71}$$

where κ_n is a weighting factor.

The test function z in Eq. (67) is called a tone detector in [Clarkson, 1997]. The test ζ for $\kappa_n = 1$ is known as the semi-coherent statistic, which has been studied since 1960 [Reed and Swerling, 1962; Lank, Reed, and Pollon, 1973]. The statistic is also known as the weighted linear predictor for different choices of κ_n, [Kay, 1989] and studied in [Clarkson, Kootsookos, and Quinn, 1994].

Following the approach of [Clarkson, 1997], the additive noise in Eq. (39a) can be arranged into a multiplicative one as:

$$z_n = \exp\{j(\theta + 2\pi f n)\}(A + \upsilon_n) \tag{72}$$

where f is an unknown signal frequency.

Since υ_n is related to the original noise w_n through multiplication by an exponent with purely imaginary argument, it is also a complex white normal random variable with the same variance.

The tone detector In Eq. (71) can be written as:

$$\zeta = e^{j2\pi f}\sum_{n=0}^{N-2} \kappa_n (A + \upsilon_{n+1})(A + \upsilon_n^*) = e^{j2\pi f} Z \tag{73}$$

It follows that, for $\kappa_n = 1$,

$$m_Z = E\{Z\} = A^2(N-1) \tag{74a}$$

$$\sigma_{Zi}^2 = E\{\mathrm{Re}(Z - m_Z)^2\} = 2\sigma^2 A^2 (2N-3) + 2\sigma^4 (N-1) \tag{74b}$$

$$\sigma_{Zq}^2 = E\{\mathrm{Im}(Z - m_Z)^2\} = 2\sigma^2 A^2 + 2\sigma^4 (N-1) \tag{74c}$$

$$E\{\mathrm{Re}(Z - m_Z)\,\mathrm{Im}(Z - m_Z)\} = 0 \tag{74d}$$

From the above equations, it is easy to see that for $A = 0$, $\sigma_{Zi}^2 = \sigma_{Zq}^2 = 2\sigma^4(N-1)$ and $\sigma_Z^2 = 4\sigma^4(N-1)$. According to Eq. (56), the output SNR of the tone detector in Eq. (71) for $\kappa_n = 1$ is:

$$(SNR)_{TD} = \frac{A^2}{2\sigma^2}\sqrt{N} = \sqrt{N}\,(SNR)_1 \tag{75}$$

which is related to the energy detector in Eq. (58) as:

$$\frac{(SNR)_{TD}}{(SNR)_{NCI\_ED}} = \sqrt{2} \tag{76}$$

Comparison of the noise-only variances shows that $\sigma_{TD}^2 = 4\sigma^4(N-1) < \sigma_{ED}^2 = 8\sigma^4 N$. In other words, $\sigma_{TD}^2 / \sigma_{ED}^2 = (N-1)/2N$. This shows that the SNR required to achieve the same detection performance by the energy detector (*i.e.*, the square law detector) is $\sqrt{2}$ higher (or 1.5 dB higher) than that required by the tone detector [Clarksons, 1997] and is also the asymptotic result of [Lank, Reed, and Pollon, 1973].

Recently, this kind of semi-coherent integration scheme has been used for differentially coherent PN code acquisition in DS-SS CDMA receivers [Zarrabiadeh and Souza, 1997] and for assisted acquisition of weak GPS signals [Choi *et al.*, 2002]. It was estimated in [Yu, 2006] that the improvement of sensitivity with such a differential combining is 1.2 dB to 1.6 dB over the noncoherent integration for $P_d = 0.1$ and $P_{fa} = 10^{-3}$, which is consistent with the above estimate. In fact, a more rigorous derivation based on the joint probability density

function of magnitude and phase for consecutive measurements was used in [Yu, 2006]. It also explained by means of Cauchy-Schwartz inequality that the noise in the tone detector is always smaller than that in the energy detector. This can be seen by comparing Eq. (45) and Eq. (71) with $A = 0$ as:

$$\begin{aligned} Var\{\zeta_{TD} \mid H_0\} &= E\{\zeta_{TD}\zeta_{TD}^* \mid H_0\} = E\{\sum_{n=0}^{N-2} w_{n+1}w_n^* (\sum_{m=0}^{N-2} w_{m+1}w_m^*)^*\} \\ &= E\{\sum_{n=0}^{N-2} w_{n+1}w_{n+1}^* w_n^* w_n\} < E\{\sum_{n=0}^{N-1} w_{n+1}w_{n+1}^* w_n^* w_n\} \\ &\le \sqrt{E\{(\sum_{n=0}^{N-1} w_{n+1}w_{n+1}^*)^2\} E\{(\sum_{n=0}^{N-1} w_n^* w_n)^2\}} \\ &= E\{(\sum_{n=0}^{N-1} w_n^* w_n)^2\} = Var\{\zeta_{ED}\zeta_{ED}^*\} \end{aligned} \quad (77)$$

If the input signal is a chirp signal (linear frequency modulation), the product terms in Eq. (67) contains a monotonic signal with a frequency of $(2\beta T_s k)$ where β is the chirping rate and $T_s k$ is the delay time. This is a beat frequency between the signal and its delayed copy, which can be estimated by performing an FFT to the sequence of conjugate products. The chirp rate can then be determined from the estimated beat frequency [Zaino *et al.*, 2000]. The test function becomes:

$$\zeta(m,k) = \sum_{n=m}^{N-1} z_n z_{n-m}^* \exp\{\frac{-j2\pi kn}{N}\} \quad (78)$$

Without noise, this is equivalent to a matched chirp filter. The performance is close to the coherent integration when the SNR is large. However, at low SNR, signal suppression can occur.

It is interesting to note that the test function specified in Eq. (78) is similar in structure to the cyclic autocorrelation function [Gardner, Napolitano, and Paura, 2005] defined at frequency α for lag parameter τ as:

$$\begin{aligned} R^\alpha(\tau) &= E\{x(n+\frac{\tau}{2})x^*(n-\frac{\tau}{2})e^{-j2\pi\alpha n}\} \\ &= \frac{1}{N}\sum_{n=1}^{N} x(n+\frac{\tau}{2})x^*(n-\frac{\tau}{2})e^{-j2\pi\alpha n} \end{aligned} \quad (79)$$

As a final note, consider a symmetric window of length M+1 centered at time index n, take a delay index m that is also symmetric relative to n, and then vary it over the data window, *i.e.*, $y_{n+m}y_{n-m}^*$ for $m \in [-M/2, M/2]$. Apply the Fourier transform over these delayed conjugate products over m, in contrast to n in Eq. (78), and this leads to the discrete Wigner-Ville distribution (DWVD) defined as:

$$WV(n,k) = 2\sum_{m=-M/2}^{M/2} y_{n+m}y_{n-m}^* \exp\{\frac{-j2\pi m2k}{M+1}\} \quad (80)$$

where the index k corresponds to the frequency at $2k/T_s(M+1)$.

In addition, the similarity of the cyclic autocorrelation function, the discrete Wigner-Ville transform, and the semi-coherent integration with the radar ambiguity function may be recognized. However, the relationship between them is only superficial. As pointed in [Gardner, 1991], the concepts, theory, and applications underlying these definitions have little in common.

SIMULATION RESULTS AND ANALYSES

For the simulations presented below, the following signal model is used:

$$s_n = s_n(f_d, \phi_0, \beta) = A\exp\{j[2\pi(f_d T_s n + \beta T_s^2 n^2) + \phi_0]\} \quad (81)$$

where A is the signal amplitude, f_d is an unknown Doppler frequency, β is an unknown chirping rate, ϕ_0 is an unknown initial phase uniformly distributed between 0 and 2π, and $T_s = 1/f_s$ is the sampling interval with f_s being the sampling frequency.

To simulate a desired SNR level, the signal amplitude A is adjusted according to:

$$A = (T_s 10^{\frac{C/N_0}{10}})^{\frac{1}{2}} \quad (82)$$

where C/N_0 is the corresponding carrier to noise ratio in dB-Hz.

In the simulations, a complex noise is used in which the real and imaginary parts are real white zero-mean Gaussian with variance $\sigma^2 = 1$. Under the Nyquist rate, the signal passes through a low pass filter with an equivalent bandwidth of $\pm f_s/2$. For $T_s = 0.001$ s, $A = 1$ corresponds to $C/N_0 = 30$ dB-Hz. This is equivalent to $SNR = 10\log_{10}(A^2/\sigma^2) = 0$ dB. Similarly, $A = 0.5$ leads to $C/N_0 = 24$ dB-Hz and equivalently $SNR = -6$ dB. We will use the input signal (single measurement) SNR values to plot simulation results whenever applicable.

We generate the probability of detection (P_d) as a function of single measurement (input) SNR (varying from -30 dB to 10 dB) for a fixed probability of false alarm ($P_{fa} = 10^{-3}$). Six integration and detection schemes are compared, which are illustrated in Fig. 1. They are:

1 - Ideal Coherent: $\lambda_{CI}(\underline{z}) = \mathrm{Re}\{\sum_{n=0}^{N-1} z_n s_n^*\}$

2 - Practical Coherent with FFT: $\lambda_{CI\_FFT}(\underline{z}) = \max\{|FFT\{\underline{z}\}|\}$

3 - Non-Coherent: $\lambda_{NCI}(\underline{z}) = \sum_{n=0}^{N-1} z_n z_n^*$

4 - Semi-Coherent for First Lag: $\lambda_{SCI}(\underline{z}) = \sum_{n=0}^{N-1} z_n z_{n-1}^*$

5 - Semi-Coherent up to First N/2 Lags: $\lambda_{SCI\_N/2}(\underline{z}) = \sum_{k=1}^{N/2} \left| \sum_{n=k+1}^{N} z_n z_{n-k}^* \right|^2$

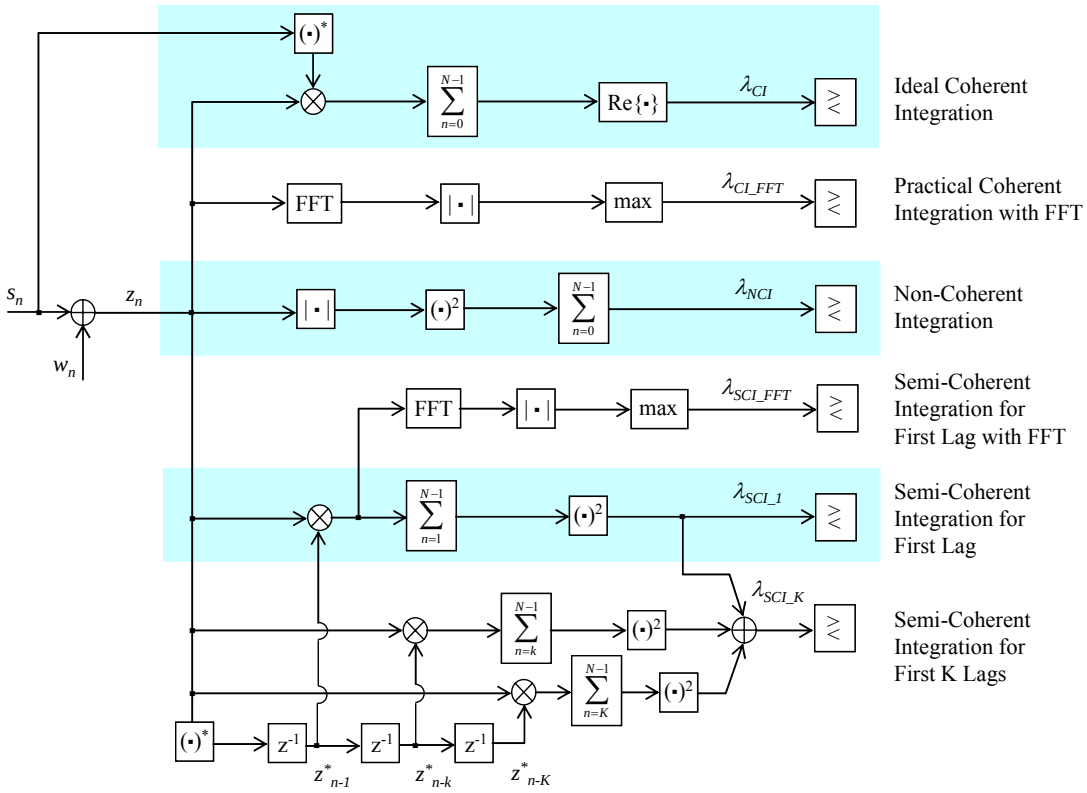

Fig. 1 – Block Diagram of Six Compared Integration Schemes

6 - Semi-Coherent for First Lag with FFT:

$$\lambda_{SCI\_FFT}(\underline{z}) = \max\{|\, FFT\{diag(\underline{z}_{1:N-1})\underline{z}^*_{0:N-2}\}\,|\}$$

where $FFT\{\underline{v}\}$ stands for an FFT operation applied to the vector $\underline{v}$ which may be zero-padded to reduce the size of frequency bin if necessary, $\max\{\underline{v}\}$ stands for finding the maximum value of $\underline{v}$, and $diag(\underline{v})$ stands for a diagonal matrix with $\underline{v}$ along the principal diagonal.

We first consider the case of a constant Doppler frequency with $\beta = 0$. The signal model reduces to

$$s_n = A\exp\{j(2\pi f_d T_s n + \phi_0)\} \tag{83}$$

and the product of the signal and the conjugate of its delay copy at lag k is:

$$s_n s^*_{n-k} = A^2 \exp\{j2\pi f_d T_s k\} \tag{84}$$

which does not depend on n and the beat frequency is therefore $f_d T_s k$ = -0.25 Hz for k = 1, T_s = 0.001 s, and f_d = -250 Hz.

We ran the six integration schemes with noise only 10,000 times so as to determine the detection threshold that could produce the desired probability of false alarm at $P_{fa} = 10^{-3}$ (*i.e.*, the threshold was crossed 10 out of 10,000 times). We then ran the six integration schemes again 10,000 times for each of the SNR values with both signal and noise present. The probability of detection was estimated as the number of runs in which the detection threshold was crossed, normalized by the total number of runs.

Figs. 2, 3, and 4 show the P_d vs. *SNR* curves for N = 20, 40, and 100, respectively. As expected, the curves are shifted toward the left (toward low SNR values) by 3 and 7 dB for the coherent integration scheme as the integration time is increased by a factor of 2 and 5, respectively. In these figures, the curves keep about the same shape and the SNR required to achieve $P_d > 0.5$ maintains the following order:

Ideal Coherent < Practical Coherent with FFT < Semi-Coherent up to First N/2 Lags < Semi-Coherent for First Lag < Semi-Coherent for First Lag with FFT < Non-Coherent

The practical coherent integration scheme implemented with FFT (*i.e.*, the green curve) is behind the ideal coherent integration (*i.e.*, the blue curve) by more or less 2 dB, that is, an integration loss of 2 dB at P_d = 0.9 for instance. The detection threshold of the practical coherent with FFT is higher than the ideal coherent to satisfy the same P_{fa}. This is because the optimization across all

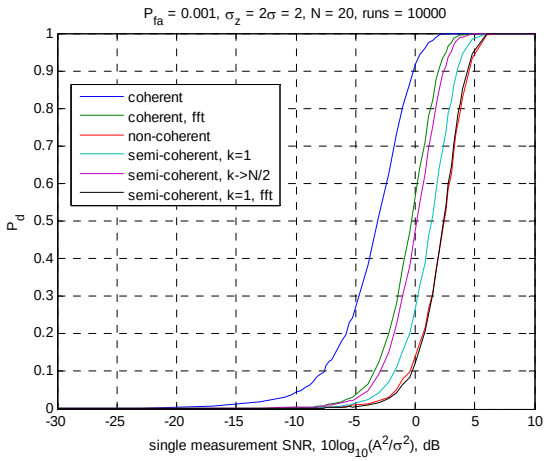

Fig. 2 – P_d vs. *SNR* for $N = 20$ ($\beta = 0$ Hz/s)

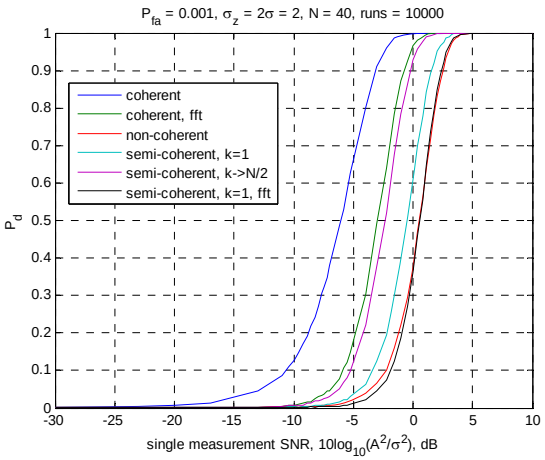

Fig. 3 – P_d vs. *SNR* for $N = 40$ ($\beta = 0$ Hz/s)

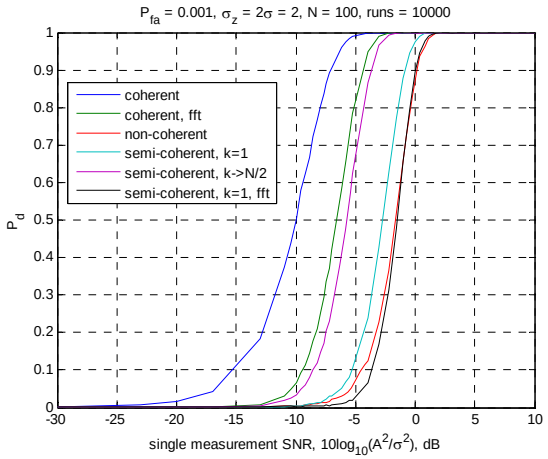

Fig. 4 – P_d vs. *SNR* for $N = 100$ ($\beta = 0$ Hz/s)

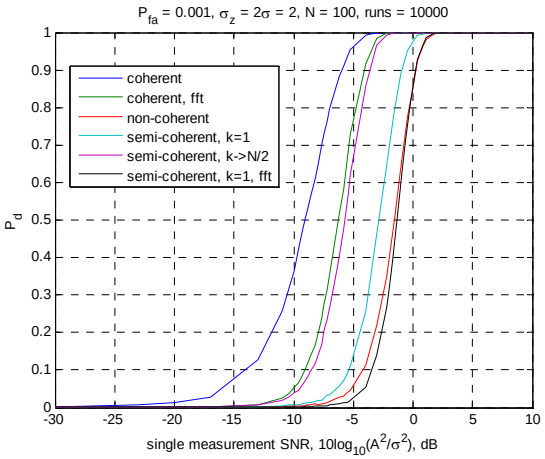

Fig. 5 – P_d vs. *SNR* for $N = 100$ ($\beta = 37.45$ Hz/s)

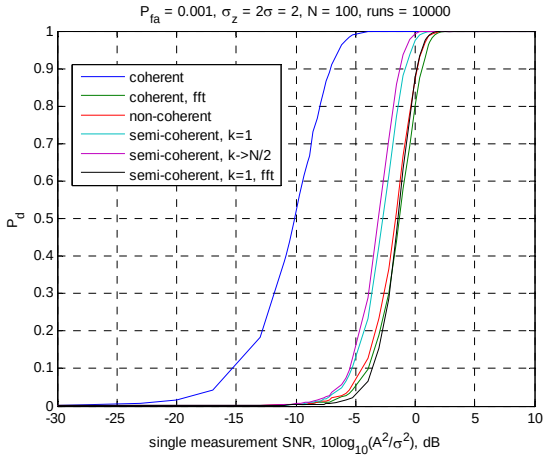

Fig. 6 – P_d vs. *SNR* for $N = 100$ ($\beta = 749$ Hz/s)

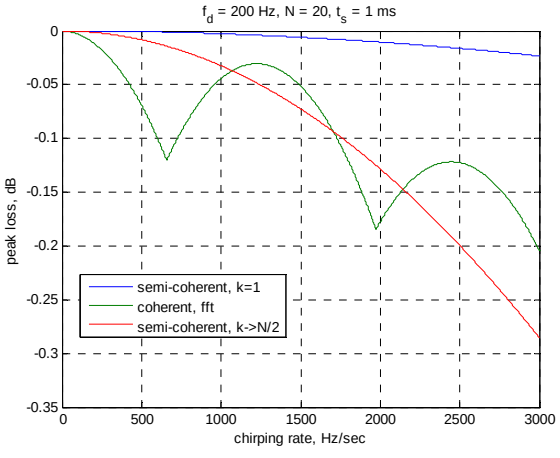

Fig. 7 – Loss of Integrated Signal Peak for $N = 20$

frequency bins tends to maximize noise. Besides, the ideal coherent only considers the noise component in the real part whereas the practical coherent with FFT takes on noise in both the real and imaginary parts via an envelope detector. When the signal frequency is between two frequency bins, an additional saddle loss may occur even though the FFT is zero-padded to four times the original size (*i.e.*, 80) to improve the frequency resolution in the simulation. The integration loss is a price to pay for not knowing the signal exactly.

The semi-coherent with FFT (the black curve) is slightly better than the non-coherent (the red curve) but both are behind the semi-coherent for first lag (the aqua curve). For the case of $\beta = 0$ with a constant Doppler frequency, the terms of conjugate products have a constant phase term. As a result, the semi-coherent with FFT produces about the same output as the semi-coherent for first lag when the signal is present. However, its detection threshold is higher for the same reasons explained above. The resulting detection performance is about the same as the non-coherent, which exhibits an integration loss of 0.9 dB at $P_d = 0.9$ as compared to the semi-coherent for first lag.

The semi-coherent up to first $N/2$ lags (the purple curve) is behind the practical coherent with FFT (the green curve) with an integration loss of about 0.3 dB for $N = 20$ and about 0.7 dB for $N = 100$ and an integration gain of 1.2 dB for $N = 20$ and 2.8 dB for $N = 100$ over the semi-coherent for first lag, respectively.

In the second simulation, we consider the case with $\beta \neq 0$. This linear frequency modulation introduces a frequency variation and will adversely affect the coherent integration. On the other hand, the product of a signal and the conjugate of its delay copy can be written as:

$$s_n s_{n-k}^* = A^2 \exp\{j2\pi f_d T_s k\} \exp\{-j\beta T_s^2 k^2\} \times \exp\{j2\pi 2\beta T_s^2 kn\} \quad (85)$$

where the first two terms do not depend on n but the third term is a monotone signal with frequency of $2\beta kT_s$. Figs. 5 and 6 show the effect of chirping rate on the detection performance of the six integration schemes for $\beta = 0$ Hz/s, 37.45 Hz/s, and $\beta = 749$ Hz/s, respectively. Both the coherent and non-coherent remain the same, unchanged by chirping rate. The semi-coherent for first lag changed very little and the semi-coherent for first lag with FFT has virtually no change. This is because the beat frequency for the conjugate products is $2\beta kT_s = 2\times749\times1\times0.001 = 1.5$ Hz/s and only causes a phase change of 0.15 cycle (54 degrees) over the integration time of 100 ms for $k = 1$ but it is 7.5 cycles for $k = 50$. It therefore has more effect on the semi-coherent up to first N/2 lags as the purple curve shifted rightwards in Figs. 5 and 6.

However, the biggest effect is on the practical coherent with FFT. Because for the coherent integration scheme, the signal frequency changed by $\Delta f = \beta NT_s = 749\times100\times0.001 = 74.9$ Hz and the signal energy was spread over 74.9 Hz/10 Hz ≈ 8 frequency bins.

Figs. 7 and 8 show the loss of integrated signal peak as a function of the chirping rate for integration time of $N = 20$ and 40, respectively. The three schemes shown, namely, the semi-coherent for the first lag (the blue curve), the practical coherent with FFT (the green curve), and the semi-coherent up to first $N/2$ lags (the red curve), all follow the same *sinc*-function in their loss. The loss of the semi-coherent up to first $N/2$ lags is faster than that of the semi-coherent for the first lag because the latter only contains one beat frequency term at $2\beta T_s$ whereas the former contains many terms at $2\beta kT_s$ for $k > 1$. The first few nulls of the *sinc*-function show up for the practical coherent with FFT.

Fig. 9 shows the loss of integrated signal peak for integration time of $N = 20$, also as a function of the chirping rate but expressed in terms of a sweep factor. The sweep factor κ is the number of frequency bins crossed over by the signal during the integration time, which is related to the chirping rate by:

$$\beta = \frac{\kappa}{(T_s N)^2},\ \kappa = 0, 1, \ldots, \frac{N}{2} - 1 \quad (86)$$

In Fig. 9, the frequency bin is $\Delta f = 50$ Hz for $N = 20$. A unit sweep factor corresponds to a chirping rate of 2500 Hz/s. Because of this large step size, the nulls are not obvious in this figure as evident in Fig. 7, which is the initial portion of Fig. 9. However, the envelope of signal peak loss is clear for the three schemes.

In the third simulation, the input SNR that is required to obtain the detection performance of ($P_d = 0.9$, $P_{fa} = 0.001$) is determined by Monte Carlo runs when the chirping rate is varied. For an integration time of N samples, the frequency bin is $1/T_s N$.

Figs. 10 and 11 show the input SNR vs. the sweep factor for N = 20 and 100, respectively. In Fig. 10, the frequency bin is $\Delta f = 50$ Hz. A unit sweep factor corresponds to a chirping rate of 2500 Hz/s. As expected the coherent (the blue curve), the non-coherent (the red curve), and the semi-coherent for first lag with FFT (the black curve) remain unchanged for different β. However, the practical coherent with FFT (the green curve) crosses (needs a larger input SNR, thus having a worse detection performance) the semi-coherent up to first N/2 lags (the purple curve) at 1.8 (3750 Hz/s). The practical coherent with FFT crosses the non-coherent at 3 (7500 Hz/s), the semi-coherent up to first $N/2$ lags crosses the non-coherent at 4 (10000 Hz/s), and the semi-coherent for first lag crosses the non-coherent at 6 (15000 Hz/s).

In Fig. 11, the frequency bin is $\Delta f = 10$ Hz. A unit sweep factor corresponds to a chirping rate of 100 Hz/s. Again, the coherent (the blue curve), the non-coherent (the red

curve), and the semi-coherent for first lag with FFT (the black curve) remain unchanged for different β. However, the practical coherent with FFT (the green curve) crosses the semi-coherent up to first $N/2$ lags (the purple curve) at 0.8 (83 Hz/s). The practical coherent with FFT crosses the non-coherent at 6.8 (680 Hz/s, which is consistent with Fig. 6), the semi-coherent up to first N/2 lags crosses the non-coherent at 17 (1700 Hz/s), and the semi-coherent for first lag crosses the non-coherent at 37 (3700 Hz/s). It is shown that the semi-coherent up to first $N/2$ lags is slightly more robust than the practical coherent with FFT against frequency change as was previously observed in [Wirth, 2001]. At a first glance, the semi-coherent for first lag with FFT behaves quite similar to the non-coherent in both detection performance and robustness against frequency changes. However, the FFT operation provides an estimate of the underlying chirping rate, which is valuable for some applications.

Comparing Fig. 11 to Fig. 10 shows that except for the coherent and non-coherent as well as the semi-coherent for first lag with FFT, all other integration schemes become more vulnerable (*i.e.*, experience larger integration loss) to changes in frequency as the integration interval gets longer. Yet, longer integration interval provides better processing gain (*i.e.*, integration improvement) as shown in Fig. 4 as compared to Figs. 2 and 3. However, a signal is more likely to be subject to changes in frequency, either due to Doppler frequency shift or to clock frequency drift, over longer intervals. It is therefore desired to develop such an integration scheme that is robust against frequency changes while providing larger integration improvements over long integration intervals.

One possible approach is to extend the semi-coherent for first lag with FFT to other lags. In other words, instead of making straight summations as in the semi-coherent up to first $N/2$ lags, FFT is used to coherently add up the conjugate products. This and other approaches are under study and will be reported in future papers [Yang *et al.*, 2007; 2008].

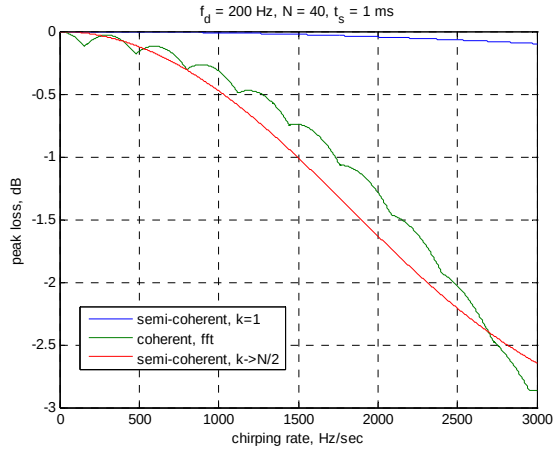

Fig. 8 – Loss of Integrated Signal Peak for $N = 40$

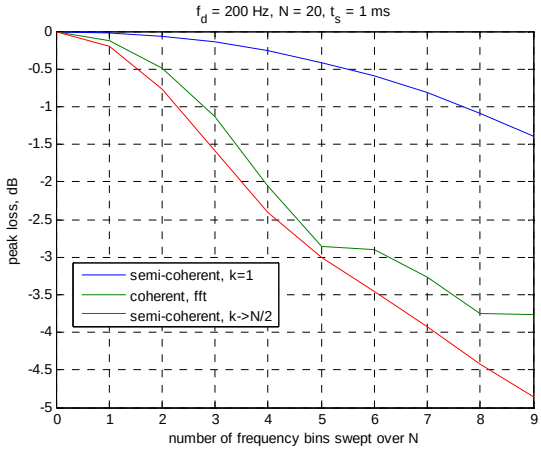

Fig. 9 – Loss of Integrated Signal Peak for $N = 20$

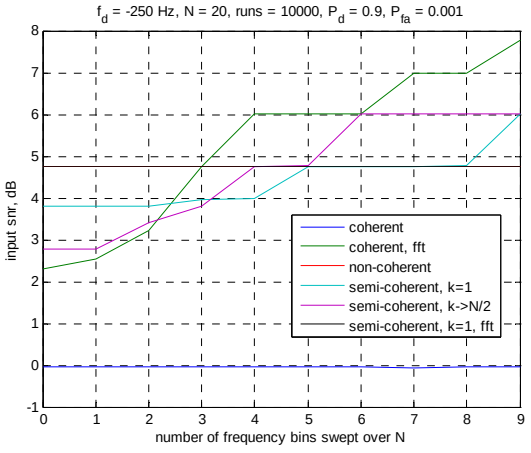

Fig. 10 – Input SNR vs. Sweep Factor for $N = 20$

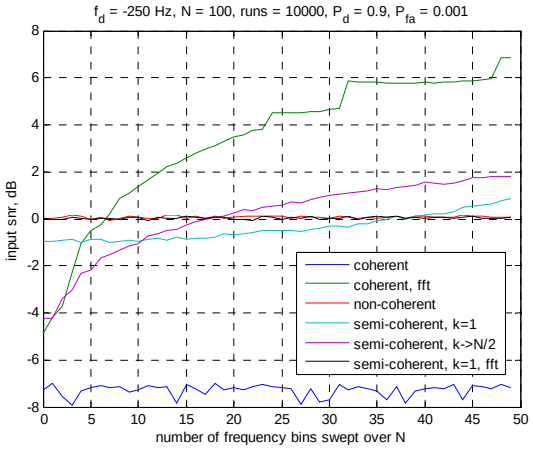

Fig. 11 – Input SNR vs. Sweep Factor for $N = 100$

CONCLUSIONS

In this paper, the coherent, non-coherent, and semi-coherent integration schemes and their variants were presented as the most appropriate approximation to the sufficient statistic of a log likelihood ratio test when the signal model was partially known to different degrees. It summarized the formulas for conditional probability density functions, probabilities of detection and false alarm as well as integration improvement factors and integration losses for these integration schemes. Results of Monte Carlo simulation were presented to compare the detection performance of these integration schemes in terms of P_d vs. *SNR* at a fixed P_{fa} for signals with constant Doppler frequency and for chirp signals. It also showed the curves of input SNR required for different chirp rates so as to maintain the same detection performance. It can be used as an easy graphic means to rank the integration schemes for different operation conditions.

ACKNOWLEDGMENTS

Research supported in part under Contracts No. FA8650-05-C-1808 and FA8650-05-C-1828, which are gratefully acknowledged.

REFERENCES

D.K. Barton, *Modern Radar System Analysis*, Artech House, Norwood, MA, 1988.

H. Choi, D.J. Cho, S.J. Yun, Y.B. Kim, and S.J. Lee, "A Novel Weak Signal Acquisition Scheme for Assisted GPS," *ION-GPS 2002*, Portland, OR, Sept. 2002.

G.R. Curry, *Radar System Performance Modeling*, Artech House, Norwood, MA, 2001.

J.V. DiFranco and W.L. Rubin, *Radar Detection*, Artech House, Norwood, MA, 1980.

I.V.L. Clarkson, "Tone and Chirp Detection Using Sums of Conjugate Products," *Proc. Australasian Workshop Signal Process. Appl.*, 189-192, December 1997

V. Clarkson, P.J. Kootsookos, and B.G. Guinn, "Analysis of the Variance Threshold of Kay's Weighted Linear Predictor Frequency Estimator," *IEEE Trans. Signal Processing*, 42(9), 2370-2379, 1994.

W.A. Gardner, "Exploitation of Spectral Redundnacy in Cyclostationary Signals," *IEEE SP Magazine*, April 1991.

W.A. Gardner, A. Napolitano, and L. Paura, "Cyclostationarity: Half a Century of Research," *Signal Processing* (Elseivier), 2005.

S.M. Kay, "A Fast and Accurate Single Frequency Estimator," *IEEE Trans. Acous. Speech Signal Proc.*, 37(12), 1987-1990, Dec. 1989.

S. M. Kay, *Fundamentals of Statistical Signal Processing, Vol. II: Detection Theory*, Prentice-Hall, Upper Saddle River, NJ, 1998.

S.A. Kassam, *Signal Detection in Non-Gaussian Noise*, Springer-Verlag, New York, 1988.

E.D. Kaplan and C.J. Hegarty (Eds.), *Understanding GPS Principles and Applications* (2nd Ed.), Artech House, Boston, MA, 2006.

G.W. Lank, I.S. Reed, and G.E. Pollon, "A Semicoherent Detection and Doppler Estimation Statistic," *IEEE Trans. Aerospace Elec. Systems*, AES-9(2), 151-165, Mar. 1973.

S.T. Lowe, "Voltage Signal-to-Noise Ratio (SNR) Nonlinearity Resulting from Incoherent Summations," *NASA-JPL TMO Progress Report 42-137*, May 1999.

P.Z. Peebles, Jr., *Radar Principles*, John Wiley & Sons, New York, 1998.

I.S. Reed and P. Swerling, "Filterless Approximations of *K*th Order to Coherent Detection," *IRE Trans. Inform. Theory*, IT-8, 196-199, Apr. 1962.

M.A. Richards, "Coherent Integration Loss due to White Gaussian Phase Noise," *IEEE Signal Processing Letters*, 10(7), July 2003.

M.A. Richards, *Fundamentals of Radar Signal Processing*, McGraw-Hill, New York, 2005.

J. Selin, "Detection of Coherent Radar Returns of Unknown Doppler Shift," *IEEE Trans. On Information Theory*, IT-511, 396-400, 1965.

M.I. Skolnik, *Introduction to Radar Systems* (3rd Ed.), McGraw-Hill, New York, 2001.

C. W., Therrien, *Decision, Estimation and Classification: An Introduction to Pattern Recognition & Related Topics*, John Wiley & Sons, New York, 1989

W.D. Wirth, *Radar Techniques Using Array Antennas*, IEE, London, UK, 2001.

C. Yang, M. Miller, T. Nguyen, and E. Blasch, "Wigner-Hough/Radon Transform for GPS Post-Correlation Integration, Submitted to *ION-GNSS'2007*, September, 2007.

C. Yang, M. Miller, T. Nguyen, and E. Blasch, "Post-Correlation Semi-Coherent Integration for High Dynamic and Weak GPS Signal Acquisition," to Be Submitted to *ION-NTM'2008*, Januray, 2008.

W. Yu, "Performance Evaluation of a Differential Approach Based Detector," I*ON-GNSS 2006*, Ft. Worth, TX, Sept. 2006.

J.C. Zaino, R.L. Bassett, T.S. Sun, J.M. Smith, E.K. Pauer, S. Kintigh, and D.W. Tufts, "An FPGA Based Adaptive Computing Implementation of Chirp Signal Detection," Google Search and Download PDF File.

M.H. Zarrabiadeh and E.S. Souza, "A Differentially Coherent PN Code Acquisition Receiver for CDMA Systems, *IEEE Trans. on Communications*, 45(11), 1456-1465, 1997.